Simulation and performance evaluation of the anoxic/anaerobic/aerobic process for biological nutrient removal

Zhen Zhou*,†, Zhichao Wu, Zhiwei Wang**, Shujuan Tang**, Guowei Gu**,
Luochun Wang*, Yingjun Wang*, and Zhiling Xin***

*School of Energy and Environmental Engineering, Shanghai University of Electric Power, Shanghai 200090, China
**State Key Laboratory of Pollution Control and Resource Reuse, College of Environmental Science and Engineering,
Tongji University, Shanghai 200092, China

Abstract−As a modified configuration of the conventional anaerobic/anoxic/aerobic (AAO) process, a novel anoxic/anaerobic/aerobic (Reversed AAO, RAAO) process has been extensively applied in domestic wastewater treatment plants (WWTP). In this study, the Activated Sludge Model No. 2d (ASM2d) and a secondary clarifier model were calibrated and applied to simulate a pilot-scale RAAO test and evaluate the operational performance of the RAAO process. For calibration of the biological model ASM2d, only four kinetic parameters were adjusted to accurately simulate in-process variations of ammonium, nitrate and phosphate. Simulation results by the calibrated model demonstrated that phosphorus accumulating organisms (PAO) in the RAAO process (0.243 gP·(gCOD)$^{-1}$) contains less poly-phosphate than the AAO process (0.266 gP·(gCOD)$^{-1}$). With the increasing mixed liquor recirculation ratio in the RAAO process, the fraction of heterotrophic biomass and autotrophic biomass both increased, whereas the PAO decreased owing to adverse effects of electron acceptors on phosphorus release and poly-hydroxy-alkanoates synthesis.

Key words: Wastewater Treatment, Biological Nutrient Removal, Simulation, Activated Sludge, Calibration

INTRODUCTION

Over the past 20 years, several biological nutrient removal (BNR) processes have been developed to eliminate phosphorus along with simultaneous nitrification-denitrification [1]. Facing complicated conversion processes and diverse organisms, mathematical simulation is a powerful tool for learning, design and process optimization of the BNR system [2-5]. In recent years, many biokinetic models have been proposed for BNR process simulation [2,6,7] and applied for various configurations, such as anaerobic/anoxic/aerobic (AAO) [7-9], University of Cape Town (UCT) [8,10], sequencing batch reactor [11], five-stage step-feed enhanced biological phosphorous removal (fsEBPR) [12], etc.

Zhang and Gao [13] developed a new-type anoxic/anaerobic/

aerobic (reversed AAO, RAAO) process (Fig. 1) with anoxic stage before anaerobic stage, and the selector was designed to control filamentous bulking and improve sludge settling characteristics [1]. The RAAO process is provided with the following advantages in comparison with conventional AAO process based on theoretical conjecture: (1) improving nitrogen removal through pre-anoxic denitrification [13]; (2) achieving "crowd microbial effect" on phosphorus removal with all activated sludge enduring both anaerobic and aerobic stages [14]; (3) ameliorating anaerobic phosphorus release by reducing electron acceptors carried by mixed liquor recirculation (MLR) and returned activated sludge (RAS) in the anoxic stage [15, 16]; (4) enhancing phosphorus uptake efficiency by preferentially aerobic utilization of poly-hydroxy-alkanoates (X_{PHA}) synthesized in the upstream anaerobic stage. The RAAO process has been exten-
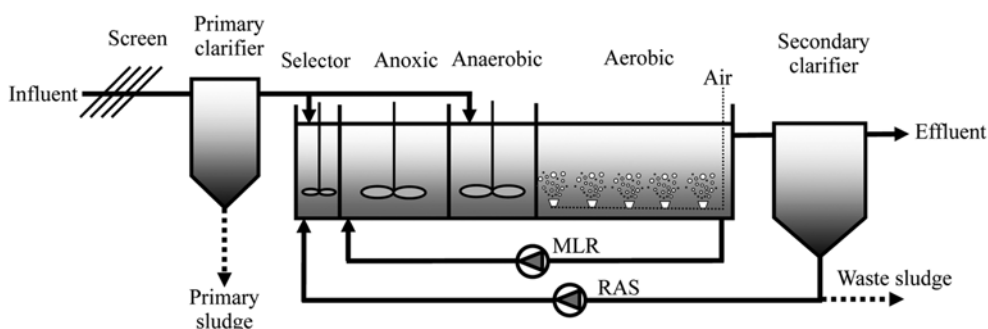

Fig. 1. Schematic flow diagram of the pilot RAAO process in the Bailonggang WWTP.

---

†To whom correspondence should be addressed.
E-mail: zhouzhen09@yahoo.com.cn

sively applied in more than 100 wastewater treatment plants (WWTP) in China and Japan now [14]. More recently, the RAAO process was designed as one operational mode (the other choice is the AAO mode) in the Bailonggang WWTP with capacity of 2,000,000 m³· d⁻¹ (Shanghai, China). Nevertheless, no information is available on mathematical modeling and performance evaluation of the RAAO process, which also requires detailed wastewater characterization and model calibration [3]. Furthermore, composite variables, including chemical oxygen demand (COD), total suspended solids (TSS), total nitrogen (TN) and total phosphorus (TP), in the effluent must be simulated to compare with permissible concentrations in various discharge standards. Therefore, the secondary clarifier model must also be calibrated before application since the considerable contribution of particulate fractions to the above-mentioned composite variables.

In this study, a pilot-scale RAAO plant in the Bailonggang WWTP was operated to investigate the applicability of Activated Sludge Model No. 2d (ASM2d) to the RAAO process. Detailed wastewater compositions are measured and used as input data of ASM2d; meanwhile, model parameters of ASM2d and the secondary clarifier model are calibrated to achieve the best simulation performance. The calibrated model is used to elucidate variations of biomass fractions as MLR varied. The results are expected to provide sound understandings of conversion processes and active biomass distributions in the RAAO process.

MATERIALS AND METHODS

1. Pilot-scale RAAO Process

The pilot plant was located at the Bailonggang WWTP, which is fed by combined sewer transported by long pipeline (about 40 km) with domestic and industrial wastewater, respectively, accounting for approximately 70% and 30% of the total flow, and consisted of a primary clarifier and an activated sludge system designed as the RAAO process (Fig. 1). The effective volumes for selector, anoxic, anaerobic and aerobic stage were 2.7, 18.9, 10.8 and 52.8 L, respectively. The secondary clarifier was 62.4 L in volume and 1.05 m in depth. The dissolved oxygen (DO) in the aerobic stage was controlled at about 2.5 mg·L⁻¹. Wastewaters after primary settler were fed into the pilot plant with constant flowrate (Q_i) of 200 L·d⁻¹. The RAS ratio (R) and MLR ratio (r) were both set to 25-100% for the RAAO process. Furthermore, step feed was applied in each test run with constant ratio of Q_i into the selector tank (f). The sludge retention time (SRT) was controlled at 15 d by sludge wastage. The main operating conditions of three test runs are summarized in Table 1.

2. Sampling Procedure and Analysis

2-1. Sampling Procedure

Grab samples were regularly collected from the influent, aerobic

stage and effluent for every 2 or 3 days. The in-process data, namely ammonium (S_{NH}), oxidized nitrogen (nitrate and nitrite, S_{NO}) and phosphate (S_{PO}) in anoxic, anaerobic and aerobic stages, were measured once a week. 24-hour composite samples of the influent were collected twice a week for COD fractionation. The mixed liquors used for COD fractionation were aerated for about 24 hours in advance to eliminate the influence of residual biodegradable COD [17,18]. The influent COD, S_{NH}, S_{PO} and TSS were also recorded by on-line sensors with recording frequency of 15 minutes.

Measurements of COD, S_{NH}, S_{NO}, TN, S_{PO}, TP, TSS, mixed liquor suspended solids (MLSS), mixed liquor volatile suspended solids (MLVSS) and alkalinity were performed according to Chinese NEPA standard methods [19]. The sludge volume index (SVI) was determined with settled sludge volume through 30 minute settling test divided by MLSS [1]. The DO and pH were measured by a DO meter (YSI 5100, YSI Research Incorporation, USA) and a portable pH meter (PHB-1, Shanghai Sanxin Com., China), respectively.

2-2. COD Fractionation

Three different types of batch tests were carried out for COD fractionation, namely a batch test with raw wastewater only to determine heterotrophic biomass (X_H) in wastewaters, one with activated sludge and raw wastewater at low F/M (food to microorganisms) ratio of 0.03-0.05 gCOD·g⁻¹MLVSS, and one with soluble wastewater obtained by zinc sulfate coagulation and activated sludge at high F/M ratio of 0.05-0.10 gCOD·g⁻¹MLVSS [18]. The soluble biodegradable COD (SBCOD) in the coagulated wastewater was considered as the sum of fatty acids (S_A) and fermentable COD (S_F), and the S_A was measured by a titration method [20]. The nitrification process of activated sludge was inhibited by 20 mg·L⁻¹ allylthiourea in the batch test [17,21]. For all the experiments, pH and temperature were maintained in the ranges of 7.0-7.5 and 19.7-20.2 °C, respectively.

3. Models and Simulation Environment

A complete model for a WWTP is partitioned into three sub-models: the hydraulic model, the clarifier model and the biological model [22,23]. For the pilot RAAO plant, no tracer studies were performed,

Table 1. Operating conditions of the pilot RAAO process

Test runs	Duration days	R %	r %	f %	Temperature °C
1	54	100	50	50	22.2
2	35	50	50	30	17.3
3	32	25	25	30	13.5

Table 2. Statistical results of measured influent pollutants in the Bailonggang WWTP

Parameter	Mean	Range
COD (mg·L⁻¹)	269.9	153.0-385.4
S_{NH} (mg·L⁻¹)	26.80	18.13-36.28
S_{NO} (mg·L⁻¹)	0.60	0-1.90
TN (mg·L⁻¹)	34.22	23.61-45.42
S_{PO} (mg·L⁻¹)	1.56	0.49-2.37
TP (mg·L⁻¹)	3.48	2.06-4.54
Alkalinity (mg·L⁻¹)	80.0	39.1-121.2
pH	7.90	7.71-8.47
COD fraction		
S_A (%)	7.94	6.23-9.24
S_F (%)	11.92	9.35-13.86
S_I (%)	13.97	10.65-17.10
X_H (%)	18.46	11.77-22.46
X_S (%)	20.23	14.20-26.41
X_I (%)	27.48	17.33-34.34

and its hydraulic model was approximated by the "tanks-in-series" approach with each compartment represented by a separate cell [2,9]. WEST 3.7.5 (MostForWater, Kortrijk, Belgium) was chosen as the simulation software. To simulate dynamic behaviors of the RAAO process at different temperatures, a pre-compiled and modified version of ASM2d in WEST 3.7.5, ASM2dTemp, was adopted with temperature correction for the biological carbon, nitrogen and phosphorus removal. Considering the high pH values in the influent (Table 2) and effluent (7.60±0.11) of the RAAO process, the metabolisms model of glycogen accumulating organisms (GAOs) was not incorporated into the ASM2dTemp model since phosphorus accumulating organisms (PAOs, X_{PAO}) usually grow dominantly and GAOs wash out in the pH-uncontrolled condition [24] and the condition with pH higher than 7.25 [25,26]. The clarification-thickening process in the secondary clarifier was modeled according to the one-dimensional model by Takács et al. [27], and the double-exponential model was used to describe the settling velocity of activated sludge, as shown in Eq. (1):

$$v_s = v_0 e^{-\gamma_h(X-X_{min})} - v_0 e^{-\gamma_p(X-X_{min})} \ (0 \le v_s \le v_0') \tag{1}$$

where, v_s is the settling velocity of activated sludge owing to gravity, $m \cdot d^{-1}$; v_0 is the maximum theoretical settling velocity, $m \cdot d^{-1}$; v_0' is the maximum practical settling velocity, $m \cdot d^{-1}$; γ_h is the hindered settling parameter, $L \cdot g^{-1}$; γ_p is the low concentration and slowly settling parameter, $L \cdot g^{-1}$; X is the concentration of MLSS, $g \cdot L^{-1}$; X_{min} is the unsettleable MLSS, $g \cdot L^{-1}$.

4. Model Calibration

Model calibration is an important step in any simulation effort to fit a certain set of data obtained from a WWTP under study through the estimation of model parameters [3]. In this study, model calibration was conducted for two sub-models: the biological model ASM2d and the secondary clarifier model. Two approaches were available for model calibration: the system engineering approach which relies purely on mathematical optimization, and the process engineering approach based on detailed understanding of the process and the model structure [3,10,23]. The system engineering approach is inapplicable to model calibration in this case owing to its complexity, poor identifiability and strict data requirements [7,15]. Therefore, a process engineering approach was adopted for model calibration through manual adjustment of model parameters until the model fitted the available test data reasonably well.

The default parameter values of ASM2d were adopted initially as the starting point for the model calibration. Then the biological model was calibrated according to an extensively applied logical step-wise procedure [3,9,22]: (1) sludge production; (2) nitrification; (3) denitrification; (4) biological phosphorus removal. The in-process data under steady-state were chosen for model calibration because they are much more informative than the effluent concentrations [3,10].

The default set of the secondary clarifier parameters [28] is not a suitable starting point for calibration attributed to the significant fluctuations of model parameters for activated sludge with different settling characteristics [27]. To reduce the calibration effort of the secondary clarifier model, a parameter estimation protocol has been advanced with model parameters linked to SVI and operational parameters [29]. According to the parameter estimation protocol, such data as effluent flowrate (Q_e), surface area of the secondary clarifier (A) and SVI shall be collected for parameter calibration of the secondary clarifier model.

RESULTS AND DISCUSSION

1. Wastewater Characterization

Table 2 gives statistical results of the influent data during the pilot plant operation according to the method of Chinese NEPA [19]. Influent COD in the Bailonggang WWTP is significantly lower than that in the Quyang WWTP located at urban areas (300-395 mg·L^{-1}) [18], and the nutrient levels in the influent are also lower than the reported values [4,10]. The mean concentration of biodegradable COD (BCOD) in the influent was 158 mg·L^{-1}, which can meet the theoretically minimal COD requirements (151 mg·L^{-1}) for complete nitrogen and phosphorus removal based on stoichiometric calculation [1,30].

According to ASM2d, influent COD is primarily made up of six fractions: S_A, S_F, soluble inert COD (S_I), X_H, slowly biodegradable COD (X_S) and particulate inert COD (X_I). Compositions of the influent COD were calculated based on respirometric profiles (Fig. 2), and their average contributions to the total COD for the entire study period are presented in Table 2. The influent fractions did not change substantially from the average values during the entire test period. The estimated (S_A+S_F) was equal to approximately 20% of total COD, and this value corresponds well to the SBCOD data in several studies [4,21], in which the concentration of SBCOD in the wastewater constituted 15.4-23.4% of total COD. The sum of S_A and S_F is not readily biodegradable COD (S_S) but SBCOD, and the soluble rapidly hydrolysable COD, is included in the S_F since the com-
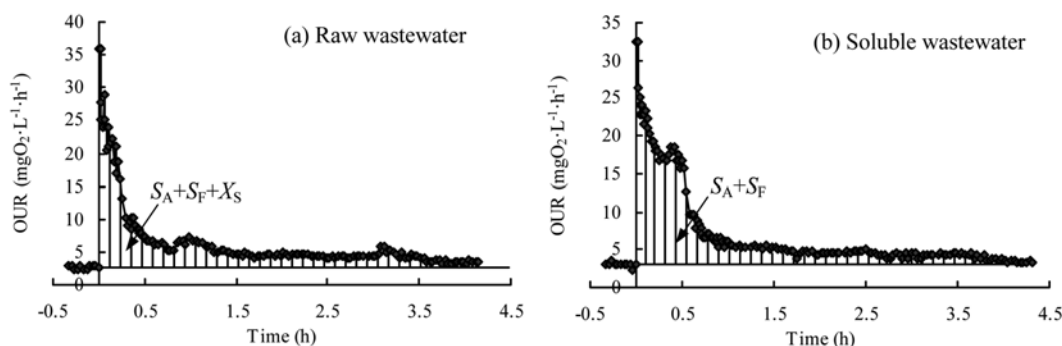

Fig. 2. Typical respirometric profiles used for the COD fractionation based on ASM2d.
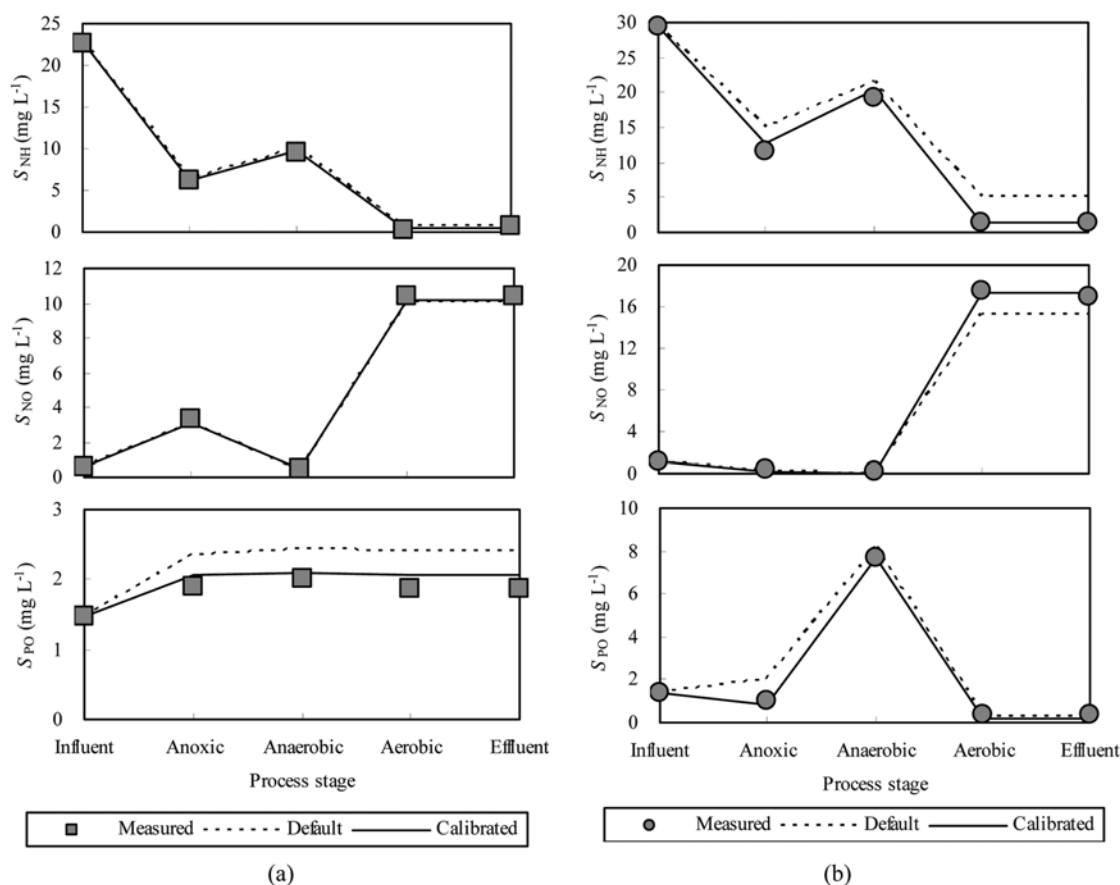
Fig. 3. Comparison of simulation results based on default and calibrated parameters. (a) Test 1, (b) Test 3.

pound can be soluble proteins, carbonhydrates, and so forth [2]. The fraction X_H in the influent accounted for about 18.5% of the total COD, higher than reported values (6.4-16.7%) [21], confirming the general tendency of active biomass growth in the sewer after about 40 km long pipeline transportation [18].

2. Model Calibration

The average in-process data of test 1 and test 3 (Fig. 3) were adopted for ASM2d model calibration. The soluble nutrient concentrations calculated by ASM2d with the default set of parameters are presented in Fig. 3 as well. As shown in Fig. 3(a) for test 1, simulation based on the standard values yielded reasonable results for S_{NH} and S_{NO} compared with the measured data; however, a large deviation is observed between the measured and calculated S_{PO} profiles in the process. As for the test 3 under low temperature (13.5 °C), the predicted concentrations of all nutrients turned out substantially deviating from measured data, especially for the S_{NH} concentration in the effluent (Fig. 3(b)). Consequently, calibration of the biokinetic model ASM2d is required for further simulation. The values of calibrated parameters with comparison to the default set of parameters are presented in Table 3.

First, the SRT and activated sludge concentrations were calibrated for each simulation by adjusting waste sludge flowrate and taking the amount of effluent TSS into account. The measured and predicted MLSS in the aerobic stage by steady-state simulation are shown in Table 4. With the measured conversion factor of 0.64 for MLVSS to MLSS, the predicted MLVSS concentrations were obtain-

Table 3. Values of the model parameters adjusted during calibration

Symbol	Unit	Default	Calibrated
Stoichiometric			
$i_{N, XI}$	$gN \cdot (gCOD)^{-1}$	0.03	0.01
$i_{N, XS}$	$gN \cdot (gCOD)^{-1}$	0.04	0.02
$i_{P, SF}$	$gP \cdot (gCOD)^{-1}$	0.01	0.005
$i_{P, XI}$	$gP \cdot (gCOD)^{-1}$	0.01	0.005
$i_{P, XS}$	$gP \cdot (gCOD)^{-1}$	0.01	0.005
Kinetic			
Autotrophic biomass (X_{AUT})			
$K_{NH, AUT}$	$mgN \cdot L^{-1}$	1.0	0.5
Heterotrophic biomass (X_H)			
$\eta_{NO, H}$	-	0.8	0.6
Phosphorus accumulating organisms (X_{PAO})			
q_{fe}	d^{-1}	3.0	1.5
$\eta_{NO, P}$	-	0.6	0.8
The Secondary clarifier model			
v_0	$m \cdot d^{-1}$	474	311.7
γ_h	$L \cdot g^{-1}$	0.576	0.339
v_0'	$m \cdot d^{-1}$	250	165
γ_p	$L \cdot g^{-1}$	2.86	7.20
f_{ns}	-	0.00228	0.00162

Table 4. Comparison of steady-state simulated results (default and calibrated) and test data*

	Test 1			Test 2			Test 3		
	Measured	Default	Calibrated	Measured	Default	Calibrated	Measured	Default	Calibrated
COD	49.6±8.2	60.3	48.3	56.8±10.7	68.0	56.5	45.0±6.4	61.4	52.4
TSS	8.1±2.8	17.1	9.0	9.5±2.6	16.5	9.1	9.2±1.3	16.8	9.4
S_{NH}	0.39±0.30	0.72	0.36	0.64±0.29	1.17	0.58	1.40±0.27	5.04	1.45
S_{NO}	10.42±1.31	10.08	10.09	12.97±1.40	13.00	13.00	16.81±1.16	15.26	17.39
TN	11.26±1.30	11.82	11.15	14.09±1.65	15.37	14.43	19.57±2.27	21.43	19.64
S_{PO}	1.81±0.19	2.40	2.07	0.89±0.28	1.22	0.91	0.38±0.16	0.24	0.23
TP	2.09±0.21	2.68	2.22	1.05±0.24	1.67	1.15	0.52±0.20	0.70	0.47
MLSS	2256±225	2288	2286	2550±229	2503	2534	2830±209	2378	2821
MLVSS	1462±172	1464	1463	1637±150	1602	1622	1837±149	1522	1805

*All concentrations were obtained in the effluent except for MLSS and MLVSS in the aerobic stage. Unit: mg·L⁻¹

ed and listed in Table 4 as well. The relatively low MLVSS/MLSS in the Bailonggang WWTP was attributed to the high proportion of inorganic substances in influent TSS (44.7±9.3%). The simulated MLVSS and MLSS by the calibrated model were in good agreement with the measured concentrations.

On the basis of in-process measurements combined with the influent data, five conversion factors related to the nitrogen and phosphorus fractions in COD compositions were adjusted, with calibrated values listed in Table 3. The estimated nitrogen and phosphorus contents appeared to be lower than the default value [2], but were still within the typical range [20] except for $i_{P,SF}$, which is slightly lower than the cited range of 0.01-0.015. The lower nitrogen and phosphorus fractions in COD compositions are probably attributed to living habit, wastewater characteristics (combined sewer) and conversion process during long pipeline transportation [2,18]. Nevertheless, this modification was needed to obtain a good fit of the TN and TP concentrations in both influent and effluent.

The nitrification was calibrated with only one parameter - autotrophic half-saturation constant for S_{NH}, $K_{NH,AUT}$, reduced from 1.0 to 0.5 mgN·L⁻¹. Lower values of this parameter are commonly encountered in small-scale plants [9,31], which can be related to a lower diffusion limitation due to high turbulence and small flocs with comparison to full-scale conditions [2]. As for the denitrification process, the heterotrophic reduction factor for denitrification ($\eta_{NO,H}$), namely the proportion of heterotrophic biomass growing under anoxic conditions, was adjusted from 0.8 to 0.6 to improve the model predictions. A lower $\eta_{NO,H}$ value (0.55) has been determined by Ni and Yu [5], which appears to be associated with wastewaters from anaerobic sewers [2]. Therefore, the lower $\eta_{NO,H}$ value in the Bailonggang WWTP seems reasonable since the influent endures long-time anaerobic environment in the sewer system. With these calibrated parameters, the in-process S_{NH} and S_{NO} in two runs were matched very well by the model prediction (Fig. 3).

As illustrated in Fig. 3, steady-state simulation by the default model usually overestimated the S_{PO} in the anoxic and anaerobic stages, which probably results from too much acetate available. Van Veldhuizen et al. [10] also observed the phenomenon during modeling biological phosphorus and nitrogen removal in a full-scale modified UCT process. Changing the fermentation rate constant (q_{fe}) was an effective approach and usually chosen as the calibration parameter for acetate production [10,32]. In this study, q_{fe} was decreased from

3.0 to 1.5 d⁻¹, whereas the anoxic reduction factor for phosphorus uptake ($\eta_{NO,P}$) was increased from 0.6 to 0.8 (Table 3). Hence, a better prediction of in-process S_{PO} was achieved (Fig. 3).

Finally, the secondary clarifier model was calibrated based on SVI (56 mL·g⁻¹ on average) and operational parameters. Parameters X_{min}, v_0, γ_h and γ_p were estimated based on the protocol proposed by Zhou et al. [29] for secondary clarifier models. With the calibrated parameters, the simulation of effluent TSS was improved significantly in comparison with the default simulation, as shown in Table 4. The TSS prediction also improved the simulation of those relevant composite variables, e.g. COD, TP and TN (Table 4).

3. Model Validation

The model was validated under steady-state and dynamic conditions with the data originating from test 2. The relative error (RE) and average relative deviation (ARD) were introduced as a measure of the model simulation accuracy. Model validation was carried out on both effluent data and activated sludge concentrations in the aerobic stage. Table 4 shows fairly good agreements between measured and steady-state simulated data of test 2 after model calibration, and the RE value for any composition is below 10%.

As can be seen from Fig. 4, the model was able to reflect the fluctuating pattern of measured MLSS and MLVSS values in the aero-
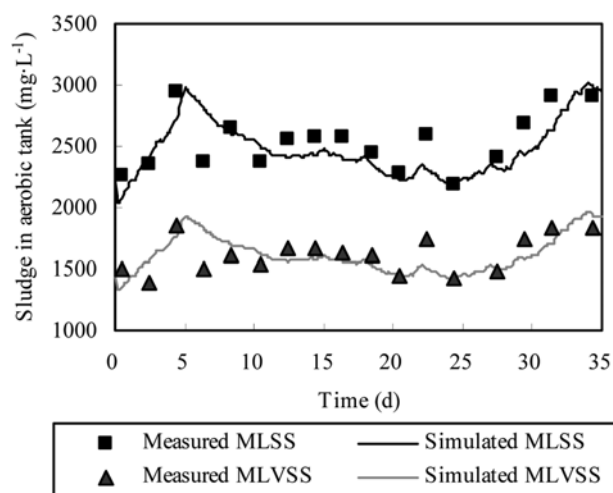

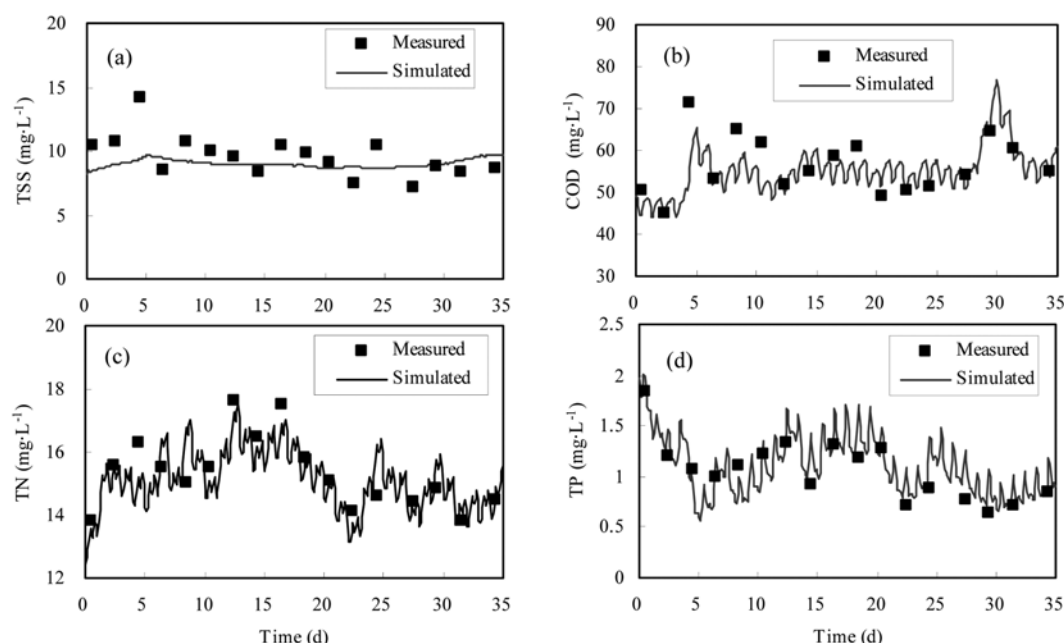**Fig. 4. Comparison of measured and simulated sludge concentrations in the aerobic stage.**

Fig. 5. Measured and simulated composite variables in the effluent. (a) TSS, (b) COD, (c) TN, (d) TP (Test 2).

bic stage. The ARD values were, respectively, 6.16% and 6.98% for MLSS and MLVSS. Moreover, the model was capable to simulate the increasing trend of activated sludge in the first 5 days and the last 10 days.

Fig. 5(a) depicts the variations of measured and simulated TSS in the effluent. The measured TSS laid between 7.2 and 14.2 mg·L^{-1}, whereas the computed ones changed from 8.2 to 9.8 mg·L^{-1}. The flux applied to the secondary clarifier fluctuated in a narrow interval (69.1-93.5 kg·d^{-1}·m^{-2}), resulting in a relatively narrow range of the simulated effluent TSS. Nevertheless, the RE value between the average measured value and steady-state simulated TSS by calibrated model was much lower than that by the default model (Table 4).

Fig. 5(b) shows the variations of measured and simulated COD values. The calibrated model was able to show the fluctuation trend in COD values, which may be attributed to the detailed influent wastewater characterization and the suitability of the calibrated secondary clarifier model [4]. In this study, the S_I composition in the influent was proportional to the influent COD [23], resulting in the undulation of simulated effluent COD because of the significant contribution of S_I to effluent COD [4,20].

We chose composite variables (TN and TP) to demonstrate the overall BNR performance. According to Fig. 5(c), simulated and experimental values of TN concentrations are consistent (ARD= 3.75%). The simulated TP values are generally in a good agreement with measured ones (Fig. 5(d)). The predicted TP values were slightly higher than the measured ones in the last 15 days of test run 2. This is partially because the temperature decreased to 15 °C in the practical test, while that used for the whole simulation was maintained constant at 17.3 °C. Since the X_{PAO} is lower-range mesophiles or possibly psychrophiles [33], phosphorus removed in the practical test was slightly higher than that in the simulated case.

4. Model-based Evaluation of the RAAO Process

The calibrated model was also used to compare steady-state operational performances of the RAAO and AAO processes and to

predict the effect of MLR ratios on BNR and biomass variations. The process variables for the simulation were as follows: step feed ratio f=50%; RAS ratio R=50%; MLR ratio r=50%; temperature 20 °C; SRT=15 d; DO=2.5 mg·L^{-1}. The average concentrations of influent compositions in Table 2 were used as the input data.

Compared to the conventional AAO process, the RAAO process yields similar carbon and nitrogen removal efficiency (data not shown here), and the greatest difference between them is the biological phosphorus removal. Fig. 6 shows the variations of cellular storage polymers (X_{PHA} and poly-phosphate (X_{PP})) of PAOs in each stage of the AAO and RAAO system. In the RAAO process, the X_{PP}/X_{PAO} increases and the X_{PHA}/X_{PAO} decreases in A1 (anoxic) stage, indicating phosphate is accumulated by denitrifying phosphorus bacteria in this stage with lower synthetic amount; a typical anaerobic phosphorus release appears in stage A1 (anaerobic) of the AAO process. In stage A2, phosphorus release amount of the RAAO pro-
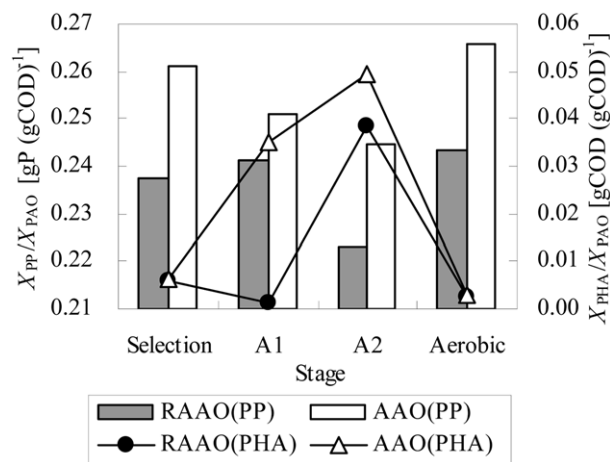

Fig. 6. Comparison on PAO stored polymers in each stage of the RAAO and AAO system.

cess is significantly higher than that of the AAO process, which is inhibited by the denitrification process in the anoxic stage. The X_{PP} content in PAOs of the AAO process is higher than that in the RAAO process, which might be attributed to the accumulative effects of the relatively higher aerobic growth levels of PAOs in the AAO process (Fig. 6). The simulated X_{PP}/X_{PAO} ratios in the aerobic tank are 0.243 gP·(gCOD)$^{-1}$ and 0.266 gP·(gCOD)$^{-1}$ for the RAAO and AAO process. These values are higher than the predictions obtained by Rieger et al. (0.12-0.15 gP·(gCOD)$^{-1}$) [34], but in substantial agreement with the simulation results of Makinia et al. (0.20-0.23

Fig. 7. Simulated TP and TN concentrations in the RAAO effluent at different MLR ratios.

gP·(gCOD)$^{-1}$) [9].

As shown in Fig. 7, effluent TN concentrations decreased from 19.65 to 13.51 mg·L^{-1} and TP concentrations increased from 0.53 to 2.00 mg·L^{-1} when MLR ratios increased from 0.0 to 1.0. According to the 1B grade of Discharge Standard of Pollutants for Municipal Wastewater Treatment Plant (GB 18918-2002, Ministry of Environmental Protection of China), effluent TN and TP concentrations of the WWTP should be no more than 20 and 1.0 mg·L^{-1}, respectively. To meet these requirements, the MLR ratio should be no more than 0.2 when RAS ratio equals to 0.5. Because the BCOD available in the influent is only slightly higher than theoretical carbon source requirements for BNR, process optimization should be performed if more stringent effluent discharge limits (e.g., 1A grade standard in GB 18918-2002 with TN<15 mg·L^{-1} and TP<0.5 mg·L^{-1}) are required.

When MLR ratio increased, percentages of X_H and X_{AUT} in the mixed liquor particulate COD (XCOD) of the RAAO system both increased (Fig. 8(a) and (b)). Fractions of X_H/XCOD and X_{AUT}/XCOD decreased in the anaerobic stage owing to the biomass lysis, and increased in the aerobic stage through the aerobic growth with oxygen supply. In the anoxic stage, the decline of these two fractions was slower with the increase of MLR ratio, and the X_{AUT}/XCOD even slightly increased when r>0.5. This is probably because the recirculation of aerobic mixed liquor to the anoxic stage leads to electron acceptors (DO and S_{NO}) inputs into the anoxic stage [16]. In the anoxic stage, X_H utilized both DO and S_{NO} as electron acceptors, while the X_{AUT} utilized only DO for its aerobic growth.

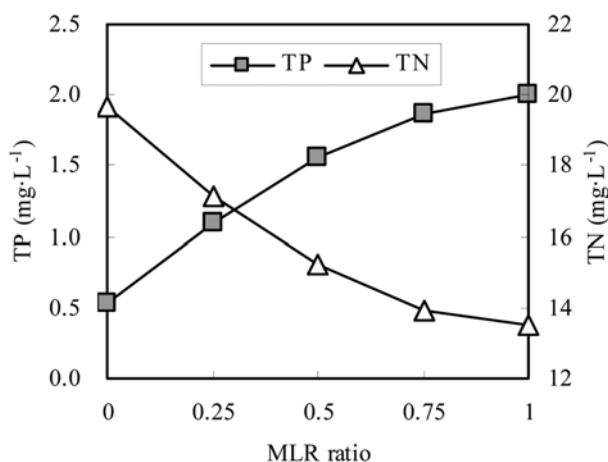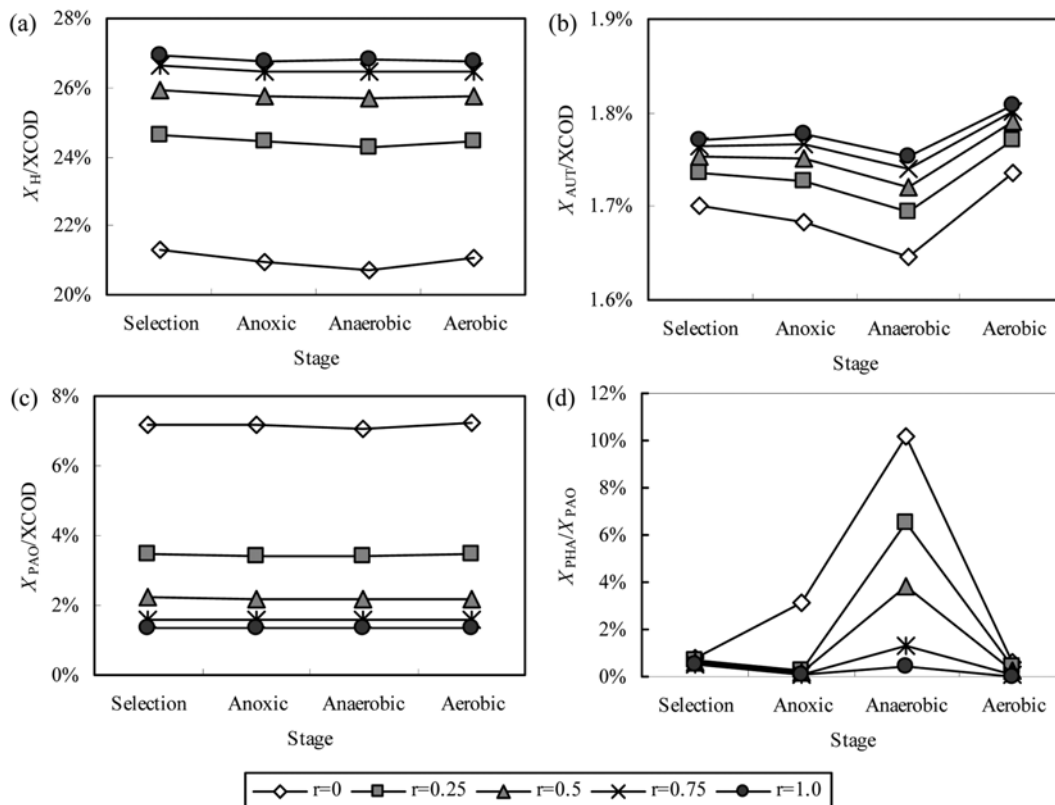As can be seen in Fig. 8(c), X_{PAO}/XCOD decreased with the en-

Fig. 8. Simulated biomass variations in each stage of the RAAO system at different MLR ratios. (a) X_H/XCOD, (b) X_{AUT}/XCOD, (c) X_{PAO}/XCOD, (d) X_{PHA}/X_{PAO}.

hancement of the MLR ratio, and fractions of X_{PAO} in the XCOD were almost the same among all stages at a certain MLR ratio. To clearly demonstrate the disturbance of MLR on X_{PAO} metabolism, X_{PHA} contents in the X_{PAO} at different MLR ratios were plotted in Fig. 8(d). When no MLR is applied on the anoxic stage, the synthesis of X_{PHA} could even occur in this stage because of the rapid consumption of electron acceptors carried out by the RAS. With the increase of returned electron acceptors, limited carbon sources might inhibit the denitrification in the anoxic stage, and the residual S_{NO} at higher MLR ratio flow into the anaerobic stage and disturb phosphorus release and X_{PHA} synthesis there [15,16]. The decrease of X_{PHA}/X_{PAO} further reduced the driving force for phosphorus uptake and X_{PAO} growth in the following aerobic stage.

CONCLUSIONS

The results of this study demonstrated that the ASM2d model could be used to simulate the behavior of a pilot-scale RAAO process to achieve BNR from a combined sewer after long pipeline transportation. With detailed wastewater characterization based on respirometric tests, the conventional influent parameters can be converted into model input data. In the biological model ASM2d, four kinetic parameters ($K_{NH,AUT}$, $\eta_{NO,H}$, q_{fe}, $\eta_{NO,P}$) together with five nitrogen and phosphorus compositions conversion factors were changed based on in-process measurements (S_{NH}, S_{NO}, S_{PO}). The secondary clarifier model was also calibrated based on SVI and operational parameters. After calibration, the model was capable of simulating the dynamics of composite variables (TSS, COD, TP and TN) in the effluent and activated sludge variations in the aerobic stage.

According to the model simulation, the X_{PP}/X_{PAO} value in the RAAO process is relatively lower than that in the AAO process based on simulation. Effluent TN decreased as a consequence of increasing MLR ratio, but the effluent TP increased. The fraction of X_H and X_{AUT} both increased with increasing MLR ratio, whereas the X_{PAO} decreased owing to the adverse effects of electron acceptors on phosphorus release and X_{PHA} synthesis. For the wastewater with limited carbon source, process optimization based on mathematical simulation is a useful tool to meet more stringent effluent discharge limits.

ACKNOWLEDGEMENTS

REFERENCES

1. G. Tchobanoglous, F. L. Burton and H. D. Stensel, *Wastewater engineering: Treatment and reuse*, Metcalf & Eddy Inc., New York (2003).
2. M. Henze, W. Gujer and T. Mino, *Activated sludge models ASM1, ASM2, ASM2D and ASM3*, IWA Scientific and Technical Report, No. 9, London (2000).
3. K. V. Gernaey, M. C. M. van Loosdrecht, M. Henze, M. Lind and S. B. Jørgensen, *Environ. Model. Softw.*, **19**, 763 (2004).
4. A. Nuhoglu, B. Keskinler and E. Yildiz, *Process Biochem.*, **40**, 2467 (2005).
5. B. J. Ni and H. Q. Yu, *Appl. Microbiol. Biotechnol.*, **77**, 723 (2007).
6. H. Siegrist, L. Rieger, G. Koch, M. Kühni and W. Gujer, *Water Sci. Technol.*, **45**, 61 (2002).
7. T. Y. Pai, *Process Biochem.*, **42**, 978 (2007).
8. J. Makinia, M. Swinarski and E. Dobiegala, *Water Sci. Technol.*, **45**, 209 (2002).
9. J. Makinia, K. H. Rosenwinkel and V. Spering, *Water Res.*, **39**, 1489 (2005).
10. H. M. van Veldhuizen, M. C. M. van Loosdrecht and J. J. Heijnen, *Water Res.*, **33**, 3459 (1999).
11. M. H. Cho, J. Lee, J. H. Kim and H. C. Lim, *Korean J. Chem. Eng.*, **27**, 925 (2010).
12. S. H. Lee, J. H. Ko, J. B. Park, J. H. Im, J. R. Kim, J. J. Lee and C. W. Kim, *Korean J. Chem. Eng.*, **23**, 203 (2006).
13. B. Zhang and T. Y. Gao, *Chin. Water and Wastewater*, **16**, 11 (2000).
14. G. Fu, B. Dong, Z. Y. Zhou and T. Y. Gao, *Chin. Water and Wastewater*, **20**, 53 (2004).
15. T. Kuba, A. Wachtmeister, M. C. M. van Loosdrecht and J. J. Heijnen, *Water Sci. Technol.*, **30**, 263 (1994).
16. T. Kuba, M. C. M. van Loosdrecht, F. A. Brandse and J. J. Heijnen, *Water Res.*, **31**, 777 (1997).
17. M. Beccari, D. Dionisi, A. Giuliani, M. Majone and R. Ramadori, *Water Sci. Technol.*, **45**, 157 (2002).
18. Z. Zhou, Z. Wu, Z. Wang, S. Tang and G. Gu, *J. Chem. Technol. Biotechnol.*, **83**, 1596 (2008).
19. Chinese NEPA, *Water and wastewater monitoring methods*, Chinese Environmental Science Publishing House, Beijing (1997).
20. P. J. Roeleveld and M. C. M. van Loosdrecht, *Water Sci. Technol.*, **45**, 77 (2002).
21. P. Ginestet, A. Maisonnier and M. Spérandio, *Water Sci. Technol.*, **45**, 89 (2002).
22. J. J. W. Hulsbeek, J. Kruit, P. J. Roeleveld and M. C. M. van Loosdrecht, *Water Sci. Technol.*, **45**, 127 (2002).
23. G. Sin, S. W. H. van Hulle, D. J. W. De Pauw, A. van Griensven and P. A. Vanrolleghem, *Water Res.*, **39**, 2459 (2005).
24. S. K. Park, M. W. Lee, D. S. Lee and J. M. Park, *Stud. Surf. Sci. Catal.*, **159**, 401 (2006).
25. C. D. M. Filipe, G. T. Daigger and C. P. L. Grady Jr, *Water Environ. Res.*, **73**, 213 (2001).
26. T. Zhang, Y. Liu and H. H. Fang, *Biotechnol. Bioeng.*, **92**, 173 (2005).
27. I. Takács, G. G. Patry and D. Nolasco, *Water Res.*, **25**, 1263 (1991).
28. J. B. Copp, *The COST simulation benchmark: Description and simulator manual*, Office for Official Publication of the European Community, Luxembourg (2002).
29. Z. Zhou, Z. Wu, G. Gu and Z. Wang, *Asia Pac. J. Chem. Eng.*, Article in press.
30. T. Kuba, M. C. M. van Loosdrecht and J. J. Heijnen, *Water Res.*, **30**, 1702 (1996).
31. G. Insel, G. Sin, D. S. Lee, I. Nopens and P. A. Vanrolleghem, *J. Chem. Technol. Biotechnol.*, **81**, 679 (2006).
32. D. Brdjanovic, M. C. M. van Loosdrecht, P. Versteeg, C. M. Hooijmans, G. J. Alaerts and J. J. Heijnen. *Water Res.*, **34**, 846 (2000).
33. T. Panswad, A. Doungchai and J. Anotai, *Water Res.*, **37**, 409 (2003).
34. L. Rieger, G. Koch, M. Kühni, W. Gujer and H. Siegrist, *Water Res.*, **35**, 3887 (2001).